THE SIMULATION OF PHOTOVOLTAIC-INTEGRATED BUILDING FACADES

Clarke J A, Johnstone C, Kelly N[#] and Strachan P A
ESRU, Dept. of Mechanical Engineering,
University of Strathclyde, Glasgow, Scotland)
([#]now at Building Research Establishment, Garston, England)

ABSTRACT

This paper describes a recent extension to the ESP-r system concerned with the simulation of facade- and roof-integrated photovoltaic modules. The algorithms are described for predicting electrical power output as a function of module characteristics, incident solar radiation and module temperature. The integration of the algorithm within ESP-r's air and power flow network models, to facilitate hybrid photovoltaic system studies, is also described. The paper concludes with a description of the outcome from an integrated appraisal of a building incorporating a photovoltaic facade.

INTRODUCTION

There is a growing interest in the use of photovoltaic-integrated (PV-I) building facades and roofs. Potentially, large surface areas are available for power production. Of greatest promise are hybrid designs, in which combined heat and electrical energy generation results in enhanced overall operational efficiency. Although there is a large amount of literature on PV systems and, increasingly, building-integrated components (PV 1995), relatively little work has been carried out on hybrid systems where use is made of the heat recovered. Recent years have seen some practical studies on the latter subject (Yang et al 1994, and IT Power 1996).

The simulation of PV-I systems requires a combined thermal/ electrical modelling approach. Electrical efficiency decreases with increasing temperature, so that ventilating the facade or roof increases power production. At the same time, the take-off of electrical power affects the thermal energy balance. Figure 1 shows the main energy flow paths.

Once endowed with a PV-I capability, a simulation model can be used to study how best to integrate the generated power and thermal energy with a building's systems for lighting, heating, ventilation etc. In this way, PV-I systems can be matched to suitable building types and their performance optimised in terms of supply-to-demand matching and system control.

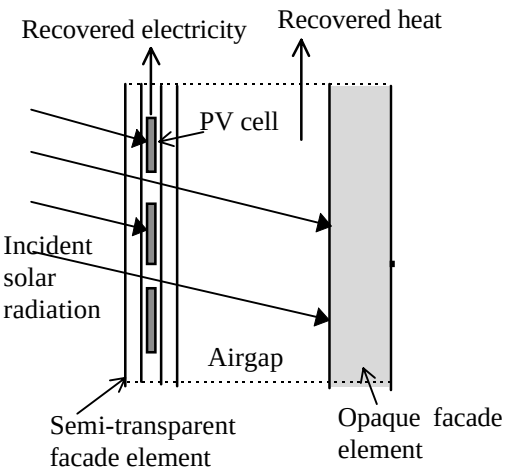

Figure 1: PV-integrated Facade

This paper describes how PV-I capabilities have been incorporated within the ESP-r system in terms of:

a) explicit models for crystalline and amorphous silicon cells,
b) the introduction of explicit power flow modelling by which alternative electrical load strategies may be studied, and
c) how the electrical and thermal flows have been numerically coupled.

The paper also reports on the results from an application of ESP-r within a study funded by the European Commission (EC) to assess the potential of PV-I systems when applied to European buildings situated in different climate contexts (Wouters et al 1996).

CALCULATION OF PV OUTPUT

The model implemented in ESP-r for calculating the power output from a PV panel is based on a set of series (n) and parallel (m) connected p-n junctions or cells as shown in Figure 2. Each junction is then represented by an equivalent circuit as shown in Figure 3.

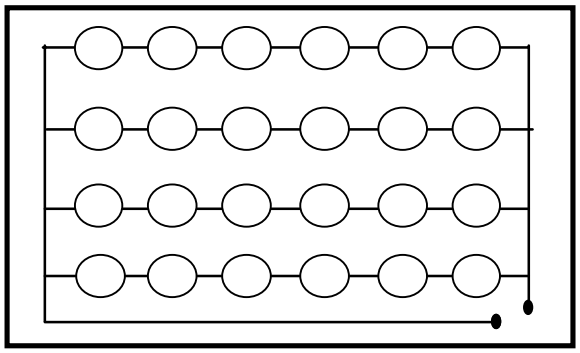

Figure 2: Example PV Panel (n=6, m=4)

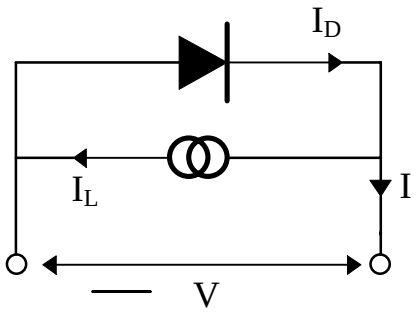

Figure 3: Equivalent Circuit for a p-n Junction with Light

For this equivalent circuit a set of equations have been derived, based on standard theory (Buresch 1983, Sorensen 1979, Millman and Grabel 1987), that allow the operation of a single junction, and hence a panel, to be simulated using data from manufacturers or experiments. The following equations apply to a panel which is operating at its maximum power point to ensure peak efficiency.

$$DF = \frac{\left(\frac{e}{kT_{ref}}\right)\left(\frac{V_{mp} - V_{oc}}{n}\right)}{ln\left(\frac{I_{sc} - I_{mp}}{I_{sc}}\right)} \quad (1).$$

$$I_o = 2^{\frac{(T-T_{ref})}{10}} \frac{-\frac{I_{sc}}{m}}{\left[exp\left(\frac{e\frac{V_{oc}}{n}}{kT_{ref}\ DF}\right) - 1\right]} \quad (2)$$

$$I_L = \frac{Q}{Q_{ref}} \frac{I_{sc}}{m} \quad (3)$$

$$1 + \frac{I_L}{I_o} = exp\left(\frac{eV_{mpp}}{kT\ DF}\right)\left[1 + \frac{eV_{mpp}}{kT\ DF}\right] \quad (4)$$

$$P = \left(V_{mpp}.I_L - V_{mpp}.I_o\left[exp\left(\frac{eV_{mpp}}{kT\,DF} - 1\right)\right]\right).n.m.N_{pnnls} \quad (5)$$

where:

V_{oc} - Open circuit voltage (at reference values, V).

I_{sc} - Short circuit current (at reference values, Amps).

V_{mp} - Voltage at maximum power point (at reference values, V).

I_{mp} - Current at maximum power point (at reference values, Amps).

Q - Incident solar radiation (W/m^2).

Q_{ref} - Reference solar radiation (usually $1000W/m^2$).

T_{ref} - Reference temperature (usually 298K).

n,m - Number of series/parallel connected cells (-).

N_{pnnls} - Number of panels (-).

DF - Diode factor (-).

I_o - Diode current (Amps).

I_L - Light generated current (Amps).

V_{mpp} - Voltage at maximum power point (at current timestep, V).

P - Panel power output (W).

e - Charge on an electron (1.60×10^{-19} C).

k - Boltzmann's constant (1.380×10^{-23} J/(K.mol)).

T - Panel temperature.

It should be noted that Equation (4) requires an iterative solution to find the maximum power point voltage. The constant, 10, in Equation (2) determines the impact of the panel temperature on output - it is normally set to 10 in the absence of experimental data.

The equations presented are those developed for crystalline silicon cells. In the case of amorphous silicon, there is evidence that other factors have an influence on the power output: an initial decrease in efficiency when exposed to outside conditions, plus temperature annealing effects and the influence of solar radiation giving rise to seasonal variations in efficiency (Dunlop et al 1995). At present, algorithms are under development so that these factors can be included in the model.

The data input requirements for the model are:

1 - Open circuit voltage at reference conditions (V).

2 - Short circuit current at reference conditions (Amps).

3 - Voltage at maximum power point at reference conditions (V).

4 - Current at maximum power point at reference conditions (Amps).

5 - Reference insolation (W/m^2).

6 - Reference temperature (K).

7 - Number of series connected cells (not panels) (-).

8 - Number of parallel connected branches (-).

9 - Number of panels in surface (-).

INTEGRATION WITHIN ESP-r

To support PV-integrated building simulation and enable heat and power utilisation studies, the PV model has been implemented within the ESP-r system. As shown in Figure 4, this coupling has three aspects:

- The assignment of special behaviour to multi-layered construction nodes in order that they can transform some part of their absorbed solar energy to electricity according to the previously described mathematical model.
- The use of an air flow network to transport heat from nodes designated as PV cells and deliver this heat to intra-building locations via heat exchangers or directly.
- The use of an electrical power flow network to allow the modelling of local electricity use and co-operative switching with the grid.

Special Materials

A *special materials* facility has been added to ESP-r whereby constructional elements can be assigned arbitrary behaviour models corresponding to advanced glazings, PV cells and the like. For the case of construction-integrated PV systems, the incident direct and diffuse solar irradiance is firstly computed on the basis of an anisotropic sky model. Where the outermost construction layers are transparent, as with PV facades, an intra-construction solar algorithm is invoked to determine the layer energy absorptions as a function of the prevailing solar incidence angle. Included within the algorithm is the effect of radiation flux retransmission back to the outside after reflection from internal room surfaces. The PV algorithm is then invoked to determine the electrical energy generated. The residual solar energy is finally re-introduced to the construction node energy balance where it acts to raise the nodal temperature (but to a lesser extent than would result in the non-PV case). The power and heat production data may then be analysed separately or fed, as inputs, to air and/or power flow sub-models which are simultaneously active.

Air and Power Flow Networks

ESP-r offers air and power flow modelling on the basis of defined networks comprising nodes and connecting components. For the case of an air flow network, nodes represent internal or boundary pressures while components represent flow resistances and the corresponding pressure drop. For a power flow network, nodes represent electrical busbars at which the components - conductors, loads and generation sources (e.g. PV power) - connect. The purpose of a network flow simulation is to determine

- the node pressures and the air exchange rates in the case of an air flow network; and
- the node voltages and phase angles, the real and reactive power flows between nodes and the system transmission losses in the case of a power flow network.

Because the numerical modelling approach is essentially the same for both networks, the following description has been abstracted to relate to both cases. Specific details on each sub-system, and the factors which differentiate them, are given

elsewhere (Clarke and Hensen 1990, Clarke et al 1997, Kelly 1997).

Each component, *i*, relates the air or current flow, f_i, through the component to the pressure or voltage potential difference, ΔP_i. Because the flow is usually non-linearly related to the potential difference across the component, the solution requires the iterative processing of a set of simultaneous equations when subjected to a given set of boundary conditions (temperature and pressure in the case of air flow; loads and power generation in the case of electricity flow). The technique employed is to assign an arbitrary pressure/voltage to each non-boundary node to enable an estimate of the air/current flow within each component. The flow residuals at each node are then computed from:

$$R_n = \sum_{j=1}^{N_{n,n}} f_j$$

where R_n is the air/current flow residual at node *n*, f_j is the flow along the *j*th connection to node *n* and $N_{n,n}$ is the total number of connections linked to node *n*.

The pressures/voltages at internal nodes are then iteratively corrected and the air/current flow residuals re-evaluated, with the procedure repeated until some convergence criterion is attained for the given time-step. The solution method is based on a Newton-Raphson technique applied to the set of simultaneous equations. Within this technique a new estimate of the vector of all node potentials (pressures/voltages), $\mathbf{P}^*$, is computed from the current potential field, **P**, via:

$$\mathbf{P}^* = \mathbf{P} - \mathbf{C}$$

where the node potential correction vector, **C**, is determined on the basis of a simultaneous solution of a Jacobian matrix which represents the nodal potential corrections in terms of the component flow partial derivatives. **C** is given by:

$$\mathbf{C} = \mathbf{R}\,\mathbf{J}^{-1}$$

where **R** is the vector of node flow residuals and $\mathbf{J}^{-1}$ is the inverse of the square Jacobian matrix (N*N for a network of N nodes) whose diagonal elements are given by:

$$J_{n,n} = \frac{\partial R_n}{\partial P_n}$$

The off-diagonal elements of **J** are given by:

$$J_{n,m} = \sum_{j=1}^{N_{n,m}} -\left(\frac{\partial f}{\partial \Delta P}\right)_j$$

where $N_{n,m}$ is the number of connections between node *n* and node *m*. For non-boundary nodes, the summation of the terms comprising each row of the Jacobian matrix are identically zero.

In the above equations, f_j and $(\partial f/\partial \Delta P)_j$ are evaluated using the latest estimate of pressure/voltage, **P**. ESP-r contains a separate subroutine for each type of flow component; this exists to return the flow rate and the partial derivative for a given potential difference. For those flow component types where an analytical expression for the partial derivative is unknown, the following numerical approximation is used.

$$\frac{\partial f}{\partial \Delta P} = \frac{f - f^{\%}}{\Delta P - \Delta P^{\%}}$$

where $^{\%}$ denotes the value in the previous iteration step.

To solve the matrix equation $\mathbf{J}\,\mathbf{C} = \mathbf{R}$ for the unknown correction vector **C**, ESP-r employs LU decomposition with implicit pivoting. The matrix **J** is decomposed to a lower triangular matrix **L** and an upper triangular matrix **U**, such that $\mathbf{L}\,\mathbf{U} = \mathbf{J}$. This decomposition is used to solve the linear set:

$$\mathbf{JC} = \mathbf{(LU)C} = \mathbf{L(UC)} = \mathbf{R}$$

by firstly solving, by forward substitution, for the vector **Y** such that $\mathbf{LY} = \mathbf{R}$ and then solving, by back substitution, $\mathbf{UC} = \mathbf{Y}$. The advantage of this method is that both substitutions are trivial. Pivoting techniques are used to assist numerical stability. Relaxation factors are included to handle the case of slow or oscillatory convergence.

APPLICATIONS

To test ESP-r's PV-I prediction capabilities, testing of a PV hybrid facade component was conducted on a PASLINK test cell (Vandaele and Wouters 1994) operating in an outdoor environment. Electrical and thermal energy data was recorded and compared with corresponding predictions. The result is shown in Figure 5. As can be seen, reasonable agreement was obtained between the recorded and predicted data for both the electrical output and the temperature of the cavity air behind the PV facade. The discrepancy between the measured and predicted power output is thought to relate to the accuracy of the solar algorithms calculating the inclined irradiance from measured horizontal irradiance data.

Given the result, and its implication that the PV algorithms were satisfactory, the model was then used to predict the thermal and electrical outputs from the test facade under typical UK winter,

spring and summer conditions. The results are summarised in Table 1.

It was now possible to model a PV-I facade as applied to the real-scale. A model was created and simulations conducted to determine the expected electrical and thermal output from a PV-hybrid facade applied to a building initially located within the UK then in a warmer European climate corresponding to northern Italy. The building chosen was the Elsa building at the EC Joint Research Centre at Ispra, Italy (Figure 4). Table 2 summarises the results. The study showed that heat recovery can make a significant impact on overall efficiency, although it should be noted that no account has been taken of fan power in these figures. Clearly, however, a central issue is the extent to which any recovered heat can be utilised, particularly in the warmer months. This will vary according to the particular design and climate. The issue is being researched in extensions to the work reported in this study (Wouters et al 1996).

CONCLUSIONS

The work described in this paper may be viewed as a contribution to truly integrated performance appraisal - in this case in relation to the thermal and electrical performance. The papers findings may be summarised thus:

- An algorithm for PV power generation has been developed and incorporated within the ESP-r system, with links established with air and power flow models.
- Reasonable agreement was found between measured and predicted thermal and electrical performance for the PV modules studied (although further work is needed for amorphous-PV modules).
- Application of the extended ESP-r system to a building incorporating a PV facade has quantified the efficiency improvements to be expected from hybrid PV systems under different European climate regimes.

Further work is underway within the EC PV-Hybrid-PAS project (Wouters et al 1996) to model a number of PV-I building facades and roofs, and assess these in terms of thermal, electrical, ventilation and lighting performance.

REFERENCES

Buresch M, Photovoltaic Energy Systems, McGraw-Hill, New York, 1983.

Clarke J A and Hensen J L M, A Fluid Flow Network Solver for Integrated Building and Plant Energy Simulation, Proc. 3rd Int. Conf. on System Simulation in Buildings, University of Liege, Belgium, pp151-167, December 1990.

Clarke J A, Evans M S, Grant A D and Kelly N, Simulation Tools for the Exploitation of Renewable Energy in the Built Environment: The EnTrack-GIS System, Proc. Building Simulation '97, Prague, 1997.

Dunlop E D, Helmke C, Jantsch M and Ossenbrink H A, Modelling Amorphous Silicon Photovoltaic Arrays Using Positive Temperature Coefficients and Standard Ambient Parameters, 13th European Photovoltaic Solar Energy Conference, Nice, pp623-626, 1995.

IT Power, PV Modules and Cladding Components, In European Solar Architecture (Eds Fitzgerald E and Lewis J O), University College, Dublin, 1996.

Kelly N, Integrated building simulation, PhD Thesis, ESRU, University of Strathclyde, To be Published, circa July 1997.

Millman J and Grabel A, Microelectronics, McGraw-Hill, New York, 1987.

PV, Proc. 13th European Photovoltaic Solar Energy Conference, Nice, 1995.

Sorensen B, Renewable Energy, Academic Press, London, 1979.

Vandaele L and Wouters P, The PASSYS Services: Summary Report, European Commission Publication, EUR 15113 EN, 1994.

Wouters P, Vandaele L and Bloem H, Hybrid Photovoltaic Building Facades: The Challenges for an Integrated Overall Performance Evaluation, 4th European Conference on Architecture, Berlin, pp579-582, 1996.

Yang H, Marshall R H and Brinkworth B J, An Experimental Study of the Thermal Regulation of a PV-Clad Building Roof, Proc. 12th European Photovoltaic Solar Energy Conference, Amsterdam, pp 1115-1118, 1994.

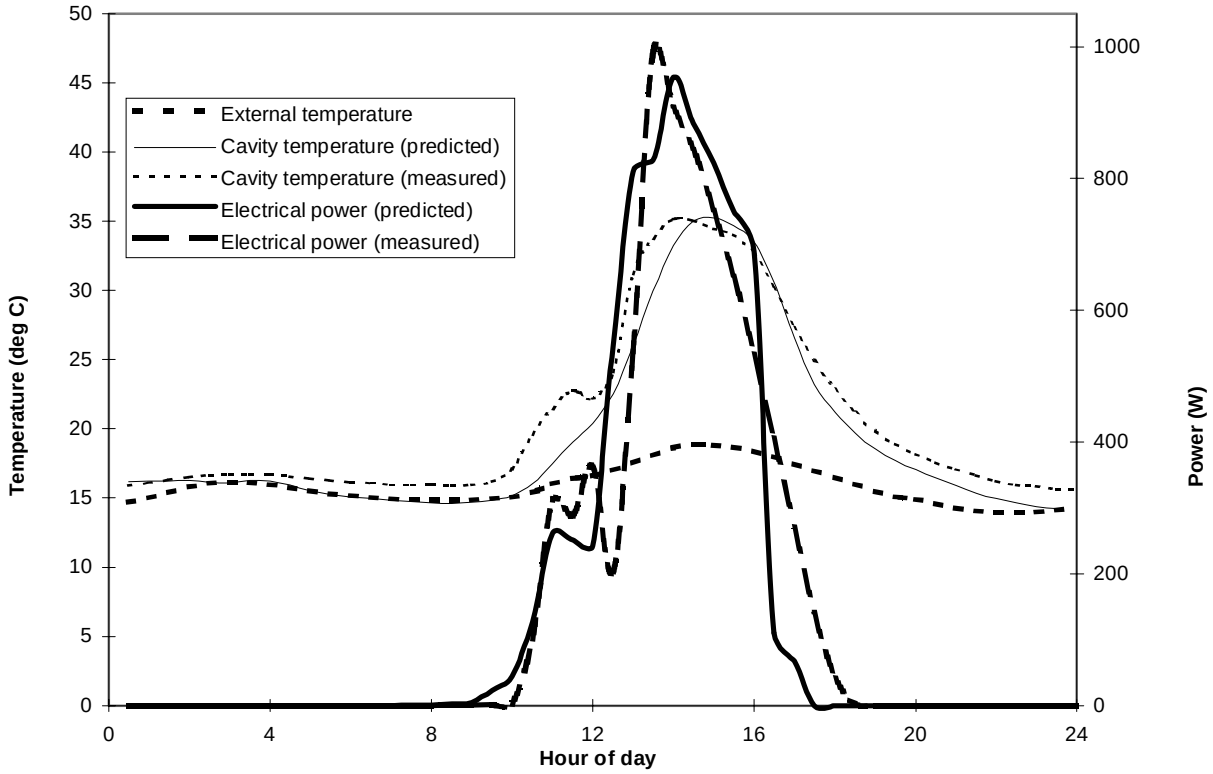

Figure 5 Comparison between recorded and predicted data

	Winter	Spring	Summer
Insolation (kWh)	26.5	132.2	211.6
Electrical Energy (kWh)	3.1	16.3	25.8
Electrical Efficiency (%)	11.7	12.3	12.2
Thermal Energy (kWh)	7.3	42.0	94.6
Combined Efficiency (%)	33.2	44.1	56.9

Table 1: Seasonal performance of PV hybrid facade

	UK (Kew)			Italy (Milan)		
	Winter	Spring	Summer	Winter	Spring	Summer
Insolation (kWh)	1606	7906	11975	5656	9704	12928
Electrical Energy (kWh)	157	837	1241	586	1026	1340
Electrical Efficiency (%)	9.8	10.6	10.4	10.4	10.6	10.4
Useful Heat (kWh)	801	2966	3053	2196	4922	300
Heat : Power ratio	5.1:1	3.5:1	2.5:1	3.7:1	4.8:1	0.22:1
Combined Efficiency (%)	59.6	48.1	35.8	49.2	61.3	12.7

Table 2: Comparison of Italian and UK PV facade performance

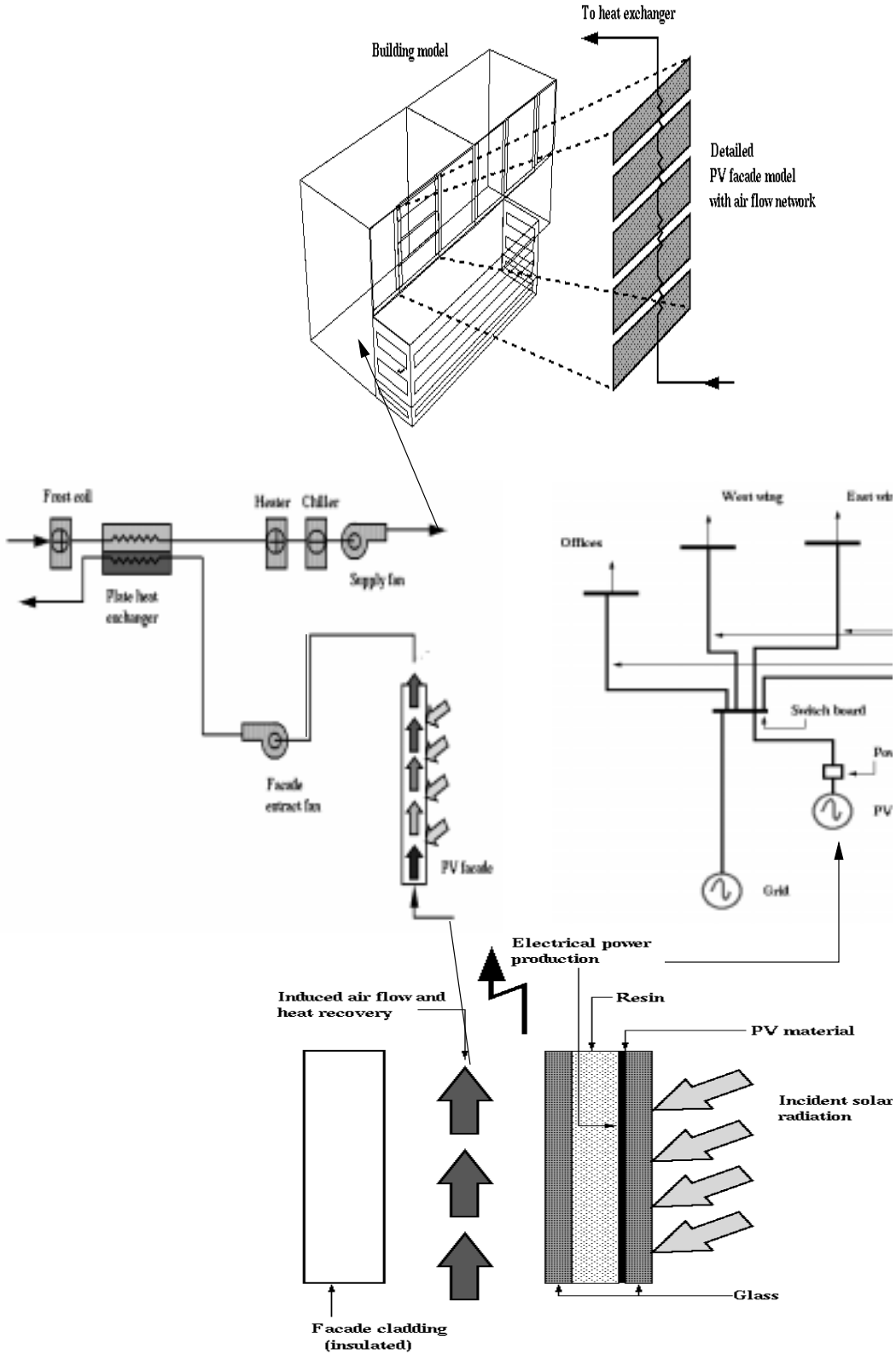

Figure 4: ESP-r's integrated PV model